

# THE DESIGN OF BEAM COLLIMATION SYSTEM FOR CSNS/RCS\*

Na Wang<sup>#</sup>, Sheng Wang, Nan Huang, Qing Qin, IHEP, Beijing, China

## Abstract

China Spallation Neutron Source (CSNS) accelerator consists of a 80 MeV linac and a 1.6 GeV Rapid Cycling Synchrotron (RCS), which is designed to produce beam power of 100 kW with a repetition rate of 25 Hz. For such a high intensity RCS, beam loss and control are of primary concern. A two-stage collimation system is designed to localize the beam losses in a restricted area, and keep the uncontrolled losses less than 1 W/m at the other part of RCS. The detailed design of the beam collimation system is presented, including the compare among different schemes. Key issues which affect the collimation efficiency are analyzed, and the collimation efficiency and beam loss distribution are studied by using the code ORBIT.

## INTRODUCTION

The CSNS [1] requires a total number of  $1.56 \times 10^{13}$  protons for the target beam power of 100 kW. In designing the RCS, one of the primary concerns is machine component radioactivation caused by uncontrolled beam losses [2]. To allow hands on maintenance, beam loss around the machine should not exceed 1 W per meter. Another important concern is the beam loss during the single turn extraction. Smaller beam emittance at extraction allows less exigent kicker strength and small beam loss at extraction. In order to achieve the low loss requirement around the ring and well constrained extraction beam extension, a two stage collimation system is designed to localize the beam losses in well shielded regions of the machine [3].

Table 1: The Main Parameters of the CSNS Ring

| Parameters           | Symbol, unit                                   | Value     |
|----------------------|--|-----------|
| Inj./Ext. energy     | $E_{inj}/E_{ext}$ , GeV                        | 0.08/1.6  |
| Circumference        | $C$ , m  | 228       |
| Beam population      | $N_p$ , $\times 10^{13}$                       | 1.56      |
| Harmonic number      | $h$  | 2         |
| Repetition frequency | $f_0$ , Hz                                     | 25        |
| Betatron tune        | $\nu_x/\nu_y$ , cm                             | 4.86/4.78 |
| Ring acceptance      | $\varepsilon$ , $\pi\text{mm}\cdot\text{mrad}$ | 540       |

Simulations are performed to predict the cleaning efficiency of the two-stage collimation system and the beam loss pattern around the CSNS ring. Both the collimators geometry and arrangement are optimized for minimizing the extent of the escaping halo. The nominal

parameters of CSNS used in the simulation are shown in Table 1.

## COLLIMATION SYSTEM DESIGN

RCS lattice is four fold structure, and it is good for provide a separate section for accommodating collimation system. The schematic layout of the RCS ring is shown in Fig. 1. The four straight sections are designed for beam injection, collimation, extraction, and RF systems, respectively. There are an 11 m and two 3.8 m dispersion free drift space. A long drift space and a short one next to it are dedicated to transverse collimators. The collimation system is located downstream of injection region. Figure 2 shows the lattice functions along a superperiod.

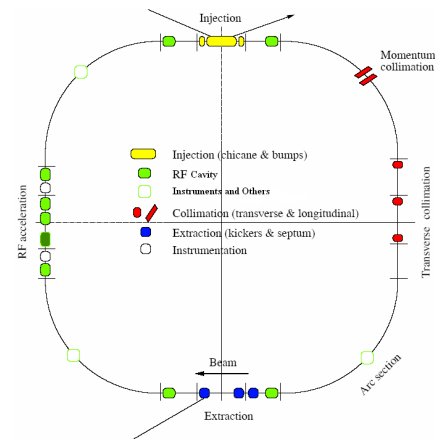


Figure 1: Schematic layout of the SNS accumulator ring.

Another straight section with large dispersion function in the arc section before the transverse collimation is dedicated to momentum collimation. As the majority of the losses in the RCS ring are due to transverse space charge halos, and longitudinal beam loss is not necessary for 100 kW beam, the momentum collimation will not be included in the primary stage, but the space is preserved for further consideration. Further studies are needed.

A set of four movable scrapers made of 0.17 mm tungsten plates acts as primary collimators for increasing the divergence of the incident halo protons. Four secondary 0.4 m long copper collimators are located downstream of primary collimator as absorbers. The layout of the collimators in the straight section is shown schematically in Fig. 2. The collimators are set to around  $350 \pi\text{mm}\cdot\text{mrad}$  for the primary and around  $400 \pi\text{mm}\cdot\text{mrad}$  for the secondary jaws. The physical aperture of the ring is designed with  $540 \pi\text{mm}\cdot\text{mrad}$  acceptance and 1% momentum deviation.

\*Work supported by the National Foundation of Natural Sciences contract 10725525 and 10605032

<sup>#</sup>wangn@ihep.ac.cn

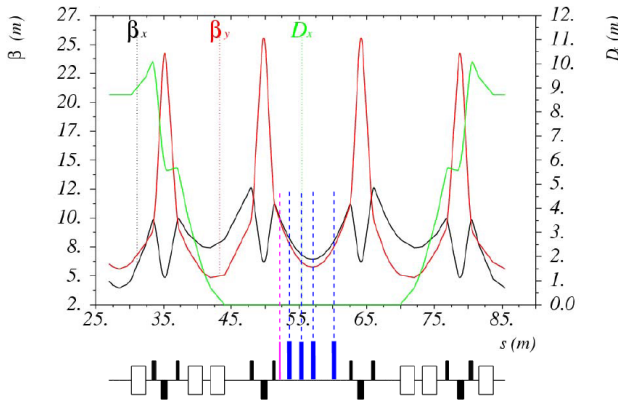


Figure 2: Lattice functions along a ring superperiod, and positions of the primary (pink) and secondary (blue) collimators.

Three different schemes have been considered for the transverse collimation system, including collimation with up-right collimator jaws, collimation with orbit bump at primary collimator, and collimation with collimators of elliptical aperture. Using the collimation systems described above, we estimate the cleaning efficiency in detail using the ORBIT code, developed at SNS [4]. The compare among different schemes is presented.

### Collimation with Upright Collimator Jaws

In this scheme, both the primary and secondary collimators consist of four plates, which are either horizontal or vertical. All collimator plates can be moved individually.

Several ORBIT simulations have been carried out to evaluate the performance of the collimation system. According to the simulation, the full beam emittance is reduced by a factor of about 30% at extraction. Figure 3 shows one example of cleaning efficiency curve. The cleaning efficiency of the system is defined as the ratio between the number of particles absorbed by the collimation system and the total number of particles lost in the RCS. The curve has been obtained by tracking 200,000 macro-particles for 4000 turns.

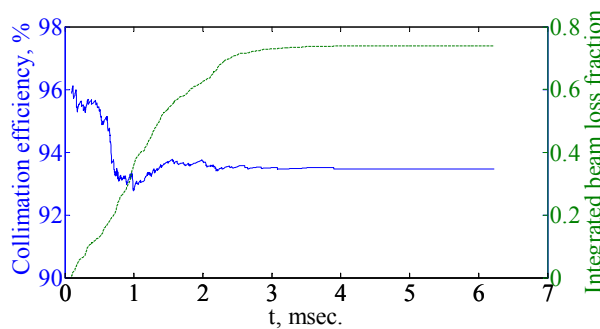


Figure 3: Collimation efficiency versus time.

The resulting efficiency in the simulation is 93.5% with 0.8% of total beam loss. The beam losses mostly occur in the first three micro seconds, either in the collimator

system or the machine apertures. The collimation efficiency varies with time as the impact parameter changes along with the expected emittance blow-up due to the transverse space charge effect.

The predicted loss distribution along RCS is given in Fig. 4, in which the green lines shows the losses to the collimation system, and the red lines represent losses to ring apertures. It is found that in the simulation, the uncontrolled beam losses at the RCS components are all constrained below 1 W/m.

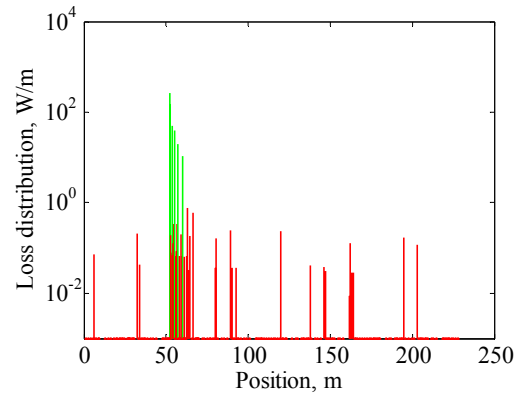


Figure 4: Predicted particle loss distribution in the CSNS RCS. The green lines represent losses to the collimators, and the red lines represent losses to ring apertures.

A summary of the loss distribution is given in Table 2. The trend in the loss distribution to the collimators is that the first collimator to absorb the largest fraction of beam, and the last collimator to absorb the smallest fraction. Over 96% of the beam is lost within the collimation straight section.

Table 2: Halo fractions absorbed in collimators and lost on the radial aperture in different ring sections

| Region/Element                   | % of Scraped Beam Lost |
|----------------------------------|------------------------|
| Scrapers                         | 0.1                    |
| First Secondary collimator       | 39.4                   |
| Second Secondary collimator      | 30.4                   |
| Third Secondary collimator       | 15.5                   |
| Fourth Secondary collimator      | 8.1                    |
| Total in the collimation section | 96.2                   |

### Collimation with Orbit Bump at Primary Collimator

In RCS, the beam emittance shrinks during the beam acceleration. So the collimation system only works at low energy range. To further clean halo particles, a method with DC orbit bump at the transverse collimators was suggested [5]. Because the DC bump will shrink with the increasing of beam magnetic rigidity during the

acceleration, it moves the beam closer to the collimators, and result in much smaller beam emittance at extraction.

During the simulation, a vertical orbit bump is located at the primary collimator, and a reduced bump factor of 0.8 is used for less ambitious collimation. By using the orbit bump method, the full-beam extraction emittance can be reduced by 20% in the vertical plane and increased by 16% in the horizontal plane. About 1.7% of the beam population are lost either at the collimator or the ring aperture. The beam loss distribution is shown in Fig. 5. The result shows larger number of beam loss locations around the ring, and some of them exceed 1 W/m. The resulting efficiency is about 90%, which is much lower than the scheme without bump.

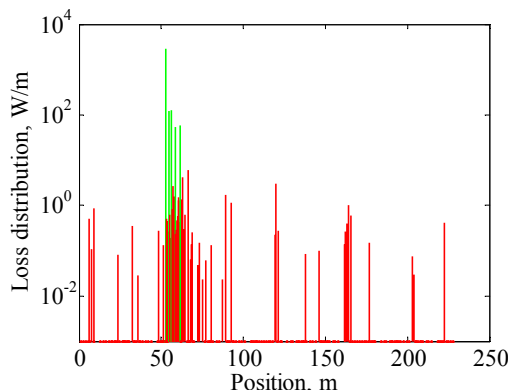


Figure 5: Predicted particle loss distribution in the CSNS RCS. The green lines represent losses to the collimators, and the red lines represent losses to ring apertures.

### Collimation with Collimators of Fixed Aperture

Collimation system with collimators of fixed elliptical aperture was also considered, i.e. of circular aperture in normalized transverse space. To realize the adjustability of the primary aperture, we use four scrapers placed 45° apart to approximate the elliptical aperture of the primary collimator.

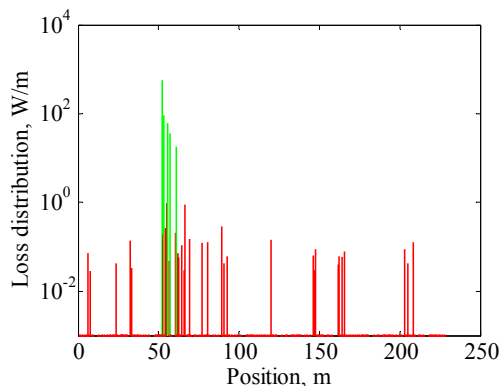


Figure 6: Predicted particle loss distribution in the CSNS RCS. The green lines represent losses to the collimators, and the red lines represent losses to ring apertures.

The beam loss distribution is shown in Fig. 6. The collimation efficiency in the simulation is 95.2% with total beam loss of 1.6%. It has a similar loss pattern as the scheme with up-right collimator jaws.

### Comparison of Different Schemes

All of the three schemes show that collimation efficiencies are better than 90%. The first scheme with up-right collimator jaws is the simplest one, and it is much flexible when changing the operation conditions. The second scheme enables more halo collimation and result in much smaller beam emittance in vertical at the extraction. As a counterpart, this contributes an emittance growth in the horizontal plane, and induces more uncontrolled beam loss around the ring. The third scheme gives better collimation efficiency as expected, but the system is less flexible. To adjust the changes of the orbit or the beam size, one can only change the collimator aperture by replacing the vacuum pipe. Besides, the modulation of the primary aperture is restricted by the fixed aperture of the secondary collimator for keeping a reasonable cleaning efficiency. Both the schemes without bump show similar beam loss patterns around the ring, and both of them fulfil the 1 W/m requirements.

According to the results obtained above, the scheme with up-right collimator jaws has been chosen for the collimation system design of CSNS/RCS.

## RELIABILITY OF THE COLLIMATION SYSTEM

The robustness of the collimation system is estimated for the collimation scheme with up-right jaws described in the previous section.

### Primary Acceptance

The collimation performance is strongly dependent on the acceptance of the primary collimators. Figure 7 shows the collimation efficiency when the primary acceptance changed from 320  $\pi$ mm·mrad to 380  $\pi$ mm·mrad, with the ratios of the acceptance of the primary and secondary collimators kept constant.

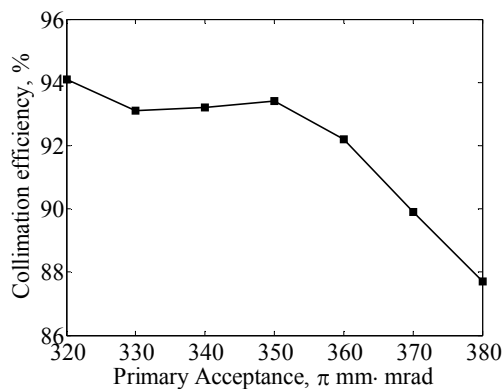


Figure 7: Dependence of the collimation efficiency on the acceptance of the primary collimator.

It can be seen that the collimation efficiency is quickly decreased when the acceptance of the primary collimator exceed  $350 \pi\text{mm}\cdot\text{mrad}$ . The higher efficiency at  $320 \pi\text{mm}\cdot\text{mrad}$  is expected due to the large impact parameter, which corresponds to a large fraction of beam losses.

### Physical Aperture

In order to ensure good collimation efficiency, an acceptance gap between the collimator and the ring physical aperture is needed. The collimation efficiency dependence on the physical aperture was estimated. The physical aperture of the ring is varied from 70% to 130% of the nominal value, and the result is shown in Fig. 8. The collimation efficiency increases with the aperture ratio, and the design value is moderate for the performance of the collimation system.

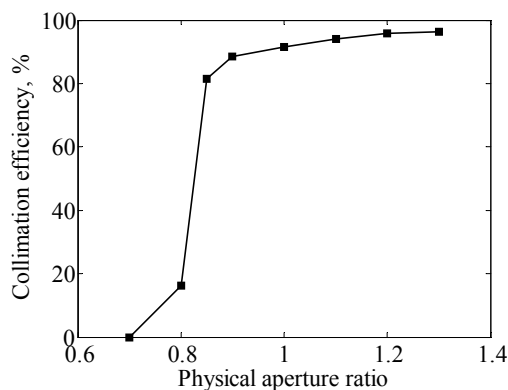


Figure 8: Dependence of the collimation efficiency on the physical aperture.

### CONCLUSION

A collimation system has been designed for the CSNS RCS. The system is composed of one primary collimator with four scrapers and four secondary collimators as absorbers. Detailed simulations of the beam collimation and multi-turn loss pattern around the RCS are performed.

With the optimal two-stage collimation system, the collimation efficiency is larger than 93%, and the maximum uncontrolled beam loss is less than 1 W/m along RCS. Three different design schemes of the collimation system have been considered taking into account collimation efficiency, beam loss pattern, extraction beam emittance as well as reliability.

All results obtained so far refer to an unperturbed machine. The ring errors or imperfect set-up of the collimation system, not yet taken into account, are expected to moderately decrease the collimation efficiency. More detailed studies including various imperfections are underway.

### ACKNOWLEDGMENTS

The authors would like to thank J.Y. Tang and the mechanical group members for their valuable discussions. Many thanks to T. Wei for his nice advices and discussions.

### REFERENCES

- [1] J. Wei et al., China Spallation Neutron Source Accelerator Design and R&D, EPAC 2006, Edinburgh, p. 366.
- [2] J. Wei, Beam Cleaning in High-Power Proton Accelerators, in Proc. of ICFA Workshop on Beam Halo Dynamics, Diagnostics, and Collimation (HALO'03), Montauk, AIP Conf. Proc., vol. 693 (2003) pp. 38-43.
- [3] T. Wei, Q. Qin, Nucl. Instr. Meth. Phys. Res. A 566 (2006) 212-217.
- [4] J. Galambos et al., ORBIT User's Manual, SNS/ORNL/AP Technical Note 011, 1999.
- [5] J.Y. Tang, Orbit bump by DC magnets and halo collimation for the RCS extraction, Nucl. Instr. Meth. Phys. Res. A 575 (2007) 328-333.